Available online at www.sciencedirect.com
ScienceDirect
Scripta Materialia 62 (2010) 770–773
Scripta MATERIALIA
www.elsevier.com/locate/scriptamat

Shear banding during cyclic deformation of sub-microcrystalline nickel

S.R. Dey,[a] L. Hollang,[a] B. Beausir,[a] E. Hieckmann[b] and W. Skrotzki[a,*]

[a] *Institut für Strukturphysik, Technische Universität Dresden, D-01062 Dresden, Germany*
[b] *Institut für Angewandte Physik, Technische Universität Dresden, D-01062 Dresden, Germany*

Received 11 December 2009; revised 2 February 2010; accepted 4 February 2010
Available online 10 February 2010

Sub-microcrystalline nickel produced by pulsed electrodeposition was investigated during cyclic deformation at high plastic strain amplitude. After a certain number of loading cycles the specimen developed a "macro" shear band at 45° with respect to the tensile axis, which acted as a crack initiator. Electron backscatter diffraction revealed that the shear band consists of relaxed grains elongated along the shear plane, showing a typical shear texture. The shear band texture was reproduced with the viscoplastic self-consistent polycrystal model using $\{1\,1\,1\}\langle 1\,1\,0\rangle$ slip systems.

Keywords: Pulsed electrodeposition; Nickel; Electron backscatter diffraction; Shear band

Increasing the strength of structural metals and alloys simply by diminishing the grain size d is a very attractive method in theory, but is usually difficult in reality. On the one hand there is no doubt that decreasing the grain size into the sub-micrometer region ($100\ \text{nm} \leqslant d \leqslant 1\ \mu\text{m}$) in most metals yields an increase in strength as predicted by the Hall–Petch law. However, in nanocrystalline metals with $d < 100$ nm the "normal" Hall–Petch behaviour may be violated by the so-called "inverse" Hall–Petch effect, even appearing during homogeneous deformation (e.g. [1]). Under special circumstances, on the other hand, sub-microcrystalline metals may behave much softer than expected in a deformation experiment simply by localizing plastic deformation, thus causing dramatic changes (e.g. relaxations) of the microstructure on a very local scale. Since Lüders [2] first observed localized slip in metal crystals in 1860, the formation of shear bands has been known to be one of the most efficient mechanisms to decrease the flow stress σ needed to initiate and/or maintain plastic deformation in metal polycrystals. The present work deals with phenomenological as well as microstructural aspects of sudden macroshear banding during cyclic deformation of sub-microcrystalline nickel as a model material for face-centred cubic metals. The quantitative analysis is based on electron backscatter diffraction (EBSD) performed in a scanning electron microscope (SEM) Zeiss ULTRA 55 equipped with a field emission gun.

An advantageous bottom-up approach to producing metals with a sub-micrometer grain size and a quite homogeneous microstructure is the technique of pulsed electrodeposition (PED). A rectangular plate of $120 \times 70 \times 5\ \text{mm}^3$ was produced through PED using a sulfamate bath without any additives for grain refinement. The pulse height was $20\ \text{mA cm}^{-2}$ and the on- and off-times of pulses were 5 and 45 ms, respectively, yielding a pulse frequency of 20 Hz. EBSD revealed that the initial microstructure of the PED nickel plate (shown further below) consisted of almost equiaxed grains in the growth plane with an average grain size of $d_{\text{EBSD}} = 160$ nm, as determined by a line intersection method. Along the growth direction (GD) the grains are elongated [3], with an overall aspect ratio of about 3. EBSD mapping did not reveal any obvious gradient along GD. Thus, the top-view EBSD maps of the sample used represent the sample's microstructure through its thickness.

Dog-bone-shaped flat specimens for cyclic deformation were cut by spark erosion, mechanically ground and then electropolished. The final size was $4.5 \times 4.5\ \text{mm}^2$ in cross-section, with a 12 mm gauge length. The cyclic deformation experiment was performed at room temperature in a servo-hydraulic MTS machine in symmetric push–pull mode under plastic strain control at a

* Corresponding author. E-mail: werner.skrotzki@physik.tu-dresden.de

1359-6462/$ - see front matter © 2010 Acta Materialia Inc. Published by Elsevier Ltd. All rights reserved.
doi:10.1016/j.scriptamat.2010.02.010

high plastic strain amplitude of $\varepsilon_{pa} = 10^{-2}$ with a constant plastic strain-rate of $\dot{\varepsilon}_p = 2 \times 10^{-5}\,s^{-1}$. Cyclic deformation experiments at much lower ε_{pa} performed on specimens stemming from the same PED nickel plate have already been published [3].

Figure 1 shows hysteresis loops during different stages of cyclic deformation. Pronounced cyclic softening is observed. The stress amplitude decreases from 1050 MPa during the first cycle to about 800 MPa after only 28 cycles. During the 29th half cycle in tension, a shear band suddenly became visible under 45° with respect to the loading axis (LA) over the whole specimen cross-section, as shown in Figure 2a (schematic diagram) and b (secondary electron image). The onset of shear band formation can be recognized easily in Figure 1. It is interesting to note that the shear plane aligns itself in a way that it contains GD. During the next (30th) cycle, the macroshear band cracked. A very similar behaviour was reported by Vinogradov and Hashimoto [4] for cyclically deformed copper processed by equal channel angular pressing (ECAP), where the cracks also initiate and propagate along the shear bands which appear if saturation is reached. In our case the crack plane contains GD and the shear direction (SD) in Figure 2a. Accordingly, the cracked side face was oriented perpendicular to GD. At that point the deformation experiment was stopped by hand and the specimen was dismounted for EBSD investigations.

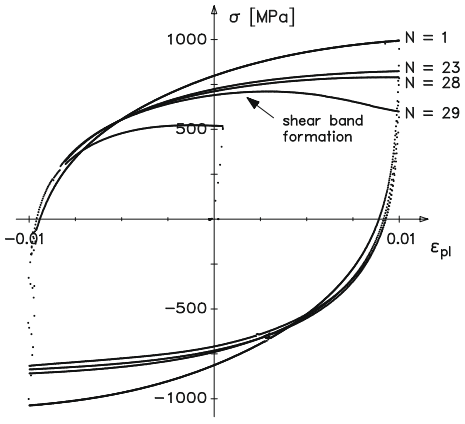

Figure 1. Hysteresis loops at different cycle numbers N, $\varepsilon_{pa} = 10^{-2}$. The shear band appeared during the 29th half cycle in tension.

The cracked side face of the specimen was ground in GD until the crack tip was reached locally, which was the case after removing about 2.3 mm of material, i.e. half of the specimen thickness. After careful electropolishing, EBSD mappings were performed on selective areas of the cracked side face as indicated by the gray squares in Figure 2a. Area (a) in the gripping region represents the initial state and area (b) the cyclically deformed but not sheared state, while area (c) contains the macroshear band, with the crack path in the lower right corner.

Figure 3a, b and c shows the orientation maps of the respective areas together with their {1 1 0}, {1 1 1} and {1 0 0} pole figures. Figure 3a shows the initial microstructure consisting of equiaxed grains of average size $d_{EBSD}(a) = 160$ nm with a weak ⟨1 1 0⟩ fibre texture along GD. The deformed area (b) shown in Figure 3b clearly has a substantially increased grain size with $d_{EBSD}(b) = 190$ nm, i.e. a 19% increase with respect to the initial state. Obviously, the increased grain size is due to grain coarsening since no change in type of texture except lowering of its strength can be noticed in the pole figures of the cyclically deformed area. There is no doubt that the process of grain coarsening is connected with ongoing pronounced dynamic recovery processes in the material, usually also leading to a reduction in the internal stresses. Indeed, the root mean square internal stresses determined by analysis of the X-ray diffraction profiles [5] dropped from 205 MPa in the initial state to 150 MPa at the end of lifetime. The cyclic rate sensitivity also decreases substantially, as was previously observed for smaller strain amplitudes [3]. We conclude that complex recovery processes are the origin of the cyclic softening visible by the decreasing stress amplitude in Figure 1.

Figure 3c shows the microstructure of the sheared region (c) with strongly elongated grains along SD. The average grain size now is $d_{EBSD}(c) = 240$ nm, i.e. a 50% increase with respect to the initial state. The trace of the crack in Figure 3c is at the lower right corner, as indicated by the sketch of area (c) in Figure 2a. Thus, the total shear band width can be estimated to be about 20–40 μm since the microstructure in the upper left corner of Figure 3c is comparable to the deformed but unsheared microstructure in Figure 3b.

Pronounced macroshear bands of similar width (≈20 μm) have been observed by Höppel et al. [6] in

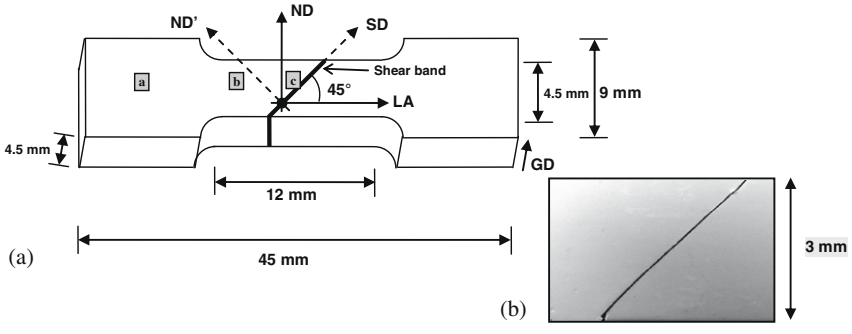

Figure 2. (a) Sketch of specimen shape with GD, ND and LA. The areas from which EBSD maps were taken are indicated by gray squares. (b) Cracked shear band on the side face in the SEM directly after dismounting the specimen.

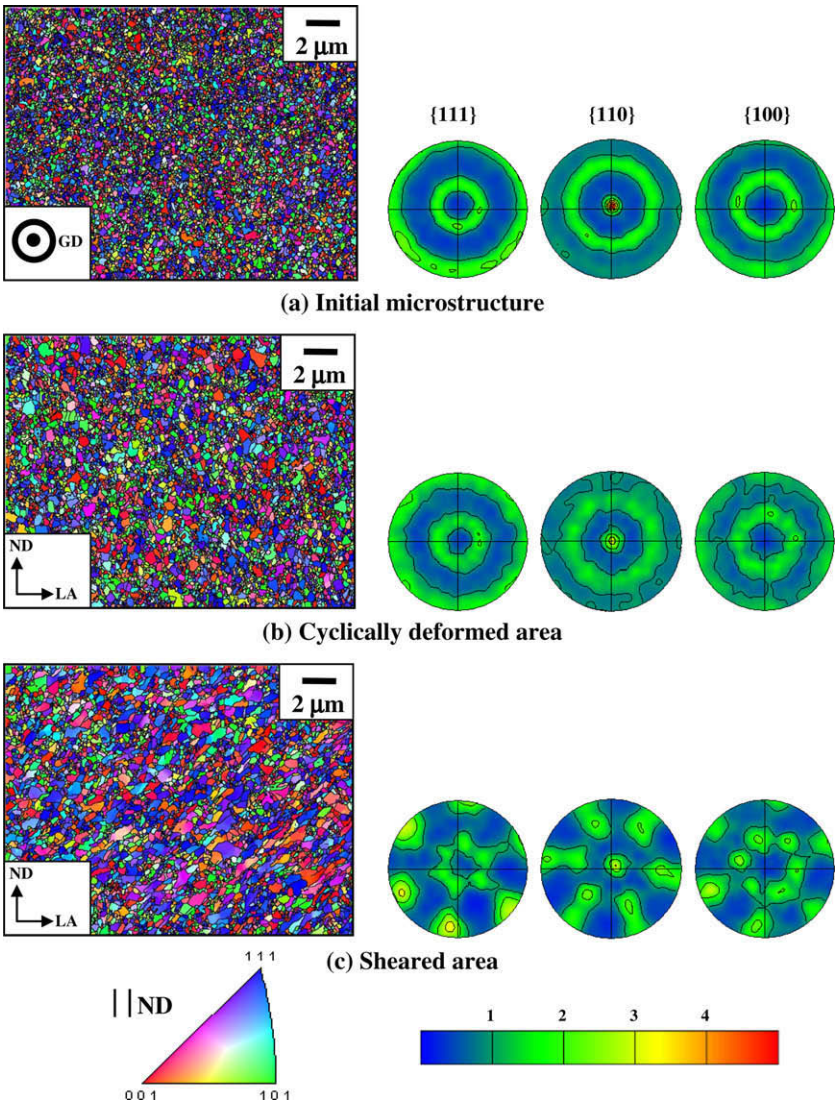

Figure 3. EBSD maps and related pole figures of (a) the initial microstructure, (b) the cyclically deformed area and (c) the sheared area. The LA, ND and GD of the pole figures are indicated in the EBSD maps. The inverse pole figure colour code parallel to ND was used in all orientation maps. (For interpretation of the references to colour in this figure legend, the reader is referred to the web version of this article.)

cyclically deformed 99.5% ECAP aluminium. They concluded that the mechanism responsible for the formation of macroscopic shear bands is an interaction of cyclically induced grain coarsening and grain rotation, both of which lead to a locally reduced strength of the material and, as a consequence, to a concentration of plastic deformation in the coarsened and/or rotated regions.

The pole figures of the sheared region appear to be quite different to the initial and the cyclically deformed regions, suggesting rotation and elongation of grains (change in texture and microstructure) during the shear process. Texture simulations of the sheared region were performed using the viscoplastic self-consistent model [7–9]. The texture measured by EBSD (≈3000 grain orientations) from the cyclically deformed area (close to the shear zone) was used as the input texture, as given in Figure 3b. It contained a weak ⟨1 1 0⟩ fibre texture along the deposition direction as was present in the initial microstructure. It is assumed that negative simple shear acts in the shear direction SD in the shear plane ND′ (see the schematic diagram of Fig. 2). The associated velocity gradient in the SD–ND′–GD reference system is:

$$\boldsymbol{L}' = \begin{pmatrix} 0 & -\dot{\gamma} & 0 \\ 0 & 0 & 0 \\ 0 & 0 & 0 \end{pmatrix}_{\mathrm{SD,ND',GD}}$$

with the shear rate $\dot{\gamma}$ positive. The shear band direction forms an angle of 45° with LA.

As the amount of shear taking place during the shear band formation is difficult to quantify, several values of shear strain were tested for the simulations to finally retain the value $\gamma = 2$. Only octahedral glide {1 1 1} ⟨1 1 0⟩ is considered in the simulation and no hardening is imposed on the slip systems. Crystallographic slip was assumed to be rate-dependent, and the constitutive law of Hutchinson [10] was employed by using three values of the strain-rate sensitivity exponent m: 0.2, 0.1 and 0.05.

Figure 4 presents the simulation results with respect to the three *m* values. The main orientation components (Fig. 3) are well reproduced by the VPSC model for all

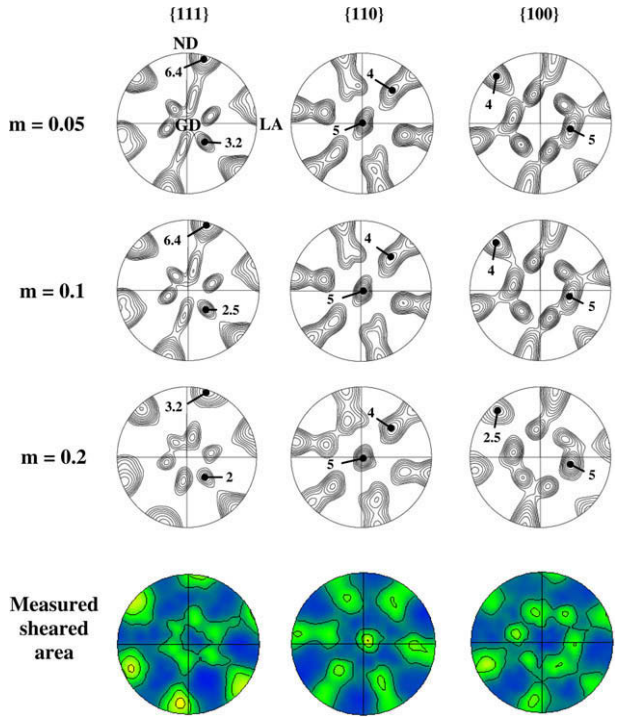

Figure 4. Texture simulations of the sheared region using the viscoplastic self-consistent model (at various strain-rate sensitivity m values and shear value $\gamma = 2$). The measured texture in the sheared area is recalled for an easier comparison. LA, ND and GD are indicated on the first pole figure.

the strain-rate sensitivity values with a preference for $m = 0.2$.

The results clearly show that cyclic loading of submicrocrystalline additive-free PED nickel at high plastic strain amplitudes ($\varepsilon_{pa} = 10^{-2}$) initially leads to pronounced cyclic softening due to grain coarsening. After a certain number of cycles, local softening promotes the development of a single macroshear band under 45° with respect to LA, initiating the fatal crack. The shear band contains strongly elongated grains exhibiting a pronounced shear texture. The good agreement between the experimental and simulated textures suggests that the amount of shear in the shear band is at least of the order of 2. There is best agreement with regard to texture strength for the highest strain-rate sensitivity value used ($m = 0.2$), suggesting an important slip activity during shear band formation [11]. It is important to note that in crystal plasticity the stress equipotentials become more and more rounded with increasing m [12–14]. As a consequence, the number of active slip systems increases, thus reducing the strength of the simulated texture. However, another reason for the difference in intensity between the experimental and simulated textures can be attributed to the fact that the present model does not take into account grain boundary processes. Indeed, grain boundary sliding usually assumed to take place in ultrafine grained materials led to a lowering of the texture intensity.

The authors gratefully acknowledge the financial support of the Deutsche Forschungs-gemeinschaft DFG, contract Sk 21/23-1. S.R.D and B.B. are grateful to the Alexander von Humboldt Foundation for their research fellowships.

[1] H. Conrad, J. Narayan, Scripta Mater. 42 (2000) 1025.
[2] W. Lüders, Dinglers polytech. J. 155 (1860) 18.
[3] L. Hollang, E. Hieckmann, C. Holste, W. Skrotzki, Mater. Sci. Eng. A 483–484 (2008) 406.
[4] A. Vinogradov, S. Hashimoto, Mater. Trans., JIM 42 (2001) 74.
[5] E. Thiele, R. Klemm, L. Hollang, N. Schell, H. Natter, R. Hempelmann, Mater. Sci. Eng. A 390 (2005) 42.
[6] H.W. Höppel, C. Xu, M. Kautz, N. Barta-Schreiber, T.G. Langdon, H. Mughrabi, in: M. Zehetbauer, R.Z. Valiev (Eds.), Nanomaterials by Severe Plastic Deformation, Wiley-VCH, Weinheim, 2002, p. 677.
[7] R. Hill, J. Mech. Phys. Solids 13 (1965) 89.
[8] A. Molinari, G.R. Canova, S. Ahzi, Acta Metall. 35 (1987) 2983.
[9] R.A. Lebensohn, C.N. Tomé, Acta Metall. 41 (1993) 2611.
[10] J.W. Hutchinson, Proc. Roy. Soc. A348 (1976) 101.
[11] B. Yang, H. Vehoff, A. Hohenwarter, M. Hafok, R. Pippan, Scripta Mater. 58 (2008) 790.
[12] L.S. Tóth, P. Gilormini, J.J. Jonas, Acta Metall. 36 (1988) 3077.
[13] B. Beausir, L.S. Tóth, K.W. Neale, Int. J. Plasticity 23 (2007) 227.
[14] L.S. Tóth, F. Qods, J.-J. Fundenberger, Z. Metallkde 96 (2005) 1038.